

Stabilizing black-box model selection with the inflated argmax

Anonymous authors

Paper under double-blind review

Abstract

Model selection is the process of choosing from a class of candidate models given data. For instance, methods such as the LASSO and sparse identification of nonlinear dynamics (SINDy) formulate model selection as finding a sparse solution to a linear system of equations determined by training data. However, absent strong assumptions, such methods are highly unstable: if a single data point is removed from the training set, a different model may be selected. In this paper, we present a new approach to stabilizing model selection with theoretical stability guarantees that leverages a combination of bagging and an “inflated” argmax operation. Our method selects a small collection of models that all fit the data, and it is stable in that, with high probability, the removal of any training point will result in a collection of selected models that overlaps with the original collection. We illustrate this method in (a) a simulation in which strongly correlated covariates make standard LASSO model selection highly unstable, (b) a Lotka–Volterra model selection problem focused on identifying how competition in an ecosystem influences species’ abundances, and (c) a graph subset selection problem using cell-signaling data from proteomics. In these settings, the proposed method yields stable, compact, and accurate collections of selected models, outperforming a variety of benchmarks.

1 Introduction

Model selection is typically formulated as a procedure to identify the model that “best” represents data from among a set of candidate models. For instance, scientists may choose among many interpretable models to identify salient variables, interactions, or policies, with the goal of developing a fundamental understanding of the natural or social phenomenon underlying experimental data. Examples of model selection include variable selection (choosing a subset of covariates from a larger pool that best explains the response variable or label), selecting a decision tree, selecting the order or memory of an autoregressive model, selecting a kernel function for a support vector machine, selecting the number of clusters in k-means, selecting the number of factors in factor analysis, and more. The issue of model selection is a common problem in a variety of domains, including bioinformatics (Saeys et al., 2007), environmental studies (Effrosynidis and Arampatzis, 2021), and psychology (Vrieze, 2012).

In this paper, we argue that constraining a procedure to return a *single* model does not adequately express any uncertainties in the model selection process, and therefore, returning a *set* of selected model(s) is more appropriate than only ever returning one. An ideal method would return a single model as often as possible while guaranteeing some degree of *stability*, i.e., the selection should not be too sensitive to small changes in the data (Yu, 2013).

Especially in model selection scenarios where the goal is to interpret the model to learn something fundamental about the studied process, trustworthiness in the results is paramount. A necessary condition for trustworthy model selection procedures is stability. Conventional methods for model selection provide *ad hoc* procedures that do not provide theoretical stability guarantees without strong assumptions on the data or model. Our goal is to provide a method that is adaptive to the underlying uncertainty of the model selection process without placing strong assumptions on the data distribution or the models themselves.

In this paper, we propose stabilizing model selection, leveraging ideas from stabilized classification (Soloff et al., 2024b), which exhibits desirable theoretical guarantees. We provide comparisons of our proposed

approach to widely used conventional model selection methods as well as explore the trade-offs of stability, accuracy, and interpretability of the model selection procedures.

1.1 Our contributions

In this work, we allow model selection procedures to return a *set* of candidate models, conveying uncertainty about which model is best while returning a single model as often as possible. We formulate a notion of model selection stability based on the idea that our claims about which model is best should remain logically consistent when we drop a small amount of data.

We develop a framework for stabilizing *black-box* model selection procedures by combining bagged model selection with the *inflated argmax* (Soloff et al., 2024b), which was formulated in the context of multiclass classification. **The key insight of this paper is that if we formulate model selection as a multi-class classification problem, where each class corresponds to one of the candidate models, then we can directly use the inflated argmax and inherit its corresponding theoretical stability guarantees for model selection, which are agnostic to the model class and data distribution.** Additionally, the stability guarantee holds even if the “true” model is not considered in the class of candidate models. We emphasize that our approach is highly generic and can be applied to many base model selection tasks, such as variable selection, constructing decision trees, selecting the order of an autoregressive model, and more.

We show empirically that the inflated argmax can improve model selection stability, and for variable selection (a special case of model selection), we similarly show this result for data with correlated covariates, a setting known to yield instabilities in standard model selection algorithms. We compare against and outperform numerous conventional model selection approaches, described in §2.2. These conventional methods, unlike our approach, are not adaptive to the underlying level of uncertainty of the model selection procedure.

2 Model selection

More formally, model selection focuses on selecting one or more models from among a set of candidate models, denoted M^+ . A *model selection procedure* is a map \mathcal{M} from data \mathcal{D} to a set of selected models $\hat{M} \subseteq M^+$. The output $\hat{M} = \mathcal{M}(\mathcal{D})$ is a nonempty subset of M^+ . If \mathcal{M} is always a singleton (i.e., $|\hat{M}| = 1$), \mathcal{M} is called *simple*.

Example. In variable selection (a special case of model selection), the data consists of n variable-response pairs $\mathcal{D} = \{(x_i, y_i)\}_{i=1}^n$, where $x_i \in \mathbb{R}^d$. We seek to identify relevant variables, so the model class $M^+ = 2^{[d]}$ is the power set of $[d] = \{1, \dots, d\}$.

The set of all candidate models M^+ can contain any class of models. For instance, in graphical model selection, M^+ is the set of all graphs G on d vertices, where an edge (j, k) in G encodes conditional dependence between variables j and k (Drton and Perlman, 2004; Friedman et al., 2008). In dynamical system identification, M^+ is a set of possible differential equations governing the dynamics underlying noisy data (Brunton et al., 2016). In econometrics, M^+ could be a collection of competing time series forecasts (Masini et al., 2023). To keep our discussion general, the model class is an abstract, countable set M^+ .

We decompose the model selection procedure \mathcal{M} into two stages

$$\mathcal{M} = \mathcal{S} \circ \mathcal{A}, \tag{1}$$

where \mathcal{A} maps data \mathcal{D} to weights $\hat{w} = \mathcal{A}(\mathcal{D}) \in \mathbb{R}^{|M^+|}$, where for each $m \in M^+$, \hat{w}_m is the weight assigned to model $m \in M^+$, and this weight can be thought of as a probability of each candidate model. The selection rule \mathcal{S} takes these weights \hat{w} as input and returns a non-empty set of selected model(s) $\hat{M} \subseteq M^+$ that provide the best fit to the data.

Algorithm 1 Bagged model selection (Breiman, 1996a;b)

input Model weighting algorithm \mathcal{A} ; data \mathcal{D} ; ensemble size B ; bag size K
for $b = 1, \dots, B$ **do**
 Construct \mathcal{D}^b by sampling uniformly (with or without replacement) K times from \mathcal{D}
 Compute model weights $\hat{w}^b = \mathcal{A}(\mathcal{D}^b)$
end for
output Ensemble weights $\hat{w} = \frac{1}{B} \sum_{b=1}^B \hat{w}^b$

2.1 Stage 1: Assigning weights to candidate models with \mathcal{A}

Base algorithm \mathcal{A} . A base algorithm \mathcal{A} is any off-the-shelf model weighting algorithm. Many model selection methods lead to weight vectors \hat{w} that place all weight on a single model (i.e., the algorithm \mathcal{A} returns only one model, so w is a vector of zeros with an entry of 1 corresponding to the selected model). Examples of such algorithms are LASSO for variable selection (Tibshirani, 1996), SINDy for model discovery for dynamical systems (Brunton et al., 2016), and graphical LASSO for graph subset selection (Friedman et al., 2008), all of which are experimentally explored in this work. A known issue of these procedures is that these algorithms can produce unstable model selections. One mechanism that has been shown to help its stability is bagging.

Bagged algorithm $\tilde{\mathcal{A}}_{K,B}$. We denote bagging a base algorithm \mathcal{A} as $\tilde{\mathcal{A}}_{K,B}$, where K is the number of samples per bag, and B is the number of bags. The output of the weighting algorithm $\tilde{\mathcal{A}}_{K,B}$ must be bounded. For simplicity, we assume that the weights can be normalized such that \hat{w} belongs to the probability simplex $\Delta_{|M^+|-1}$.¹ Bagging averages an ensemble of weight vectors fit on different randomly sampled bags — see Algorithm 1. Sampling with replacement is known as *bagging*, and sampling without replacement is known as *subbagging*.

For simple model selection procedures, the ensemble weight \hat{w}_m simply counts the fraction of bags wherein model m was selected. Even if the set of candidate models is infinite (i.e., $|M^+| = \infty$), the weights \hat{w} will have at most B nonzero entries, so bagging is still tractable. Generally, increasing the number of bags B used in $\tilde{\mathcal{A}}_{K,B}$ provides a more stability, as we empirically show in Figures 12 and 13.

2.2 Stage 2: Conventional selection rules \mathcal{S}

We discuss conventional selection approaches \mathcal{S} and their limitations.

The standard argmax. The default selection rule selects the best model(s) $\hat{M} \in \operatorname{argmax}_m \hat{w}_m$. (\hat{M} may contain more than one model in the case of exact ties for the top weight.) If the weights contain near-maximizers, the argmax can be sensitive to small perturbations of \hat{w} , meaning that a different model may be selected with a small perturbation to the training data.

Top- k . Instead of returning the very best model(s) using the argmax, an alternative is to return the top k models that receive the largest weight, where k is user-specified. Similar to the argmax, top- k fails to automatically adapt to the inherent uncertainty in the model selection process. In particular, if \hat{w} has far more than k near-maximizers, top- $k(\hat{w})$ will be unstable. On the other hand, if \hat{w} has fewer than k near-maximizers, top- k returns a set that is unnecessarily large.

Stability selection. In the context of variable selection, the stability selection method (Meinshausen and Bühlmann, 2010) selects a single model based on whether each covariate is included in the model with probability at least τ . Concretely, consider a vector of weights \hat{w} indexed by $M^+ = 2^{[d]}$, where \hat{w}_m roughly represents the probability that m is the correct model. Define the marginal variable probabilities $\hat{\Pi}_j = \sum_{m \subseteq [d]: j \in m} \hat{w}_m$, for $j = 1, \dots, d$, where $j \in m$ corresponds to variable j being included in model m . Stability selection returns

$$\operatorname{ip}_\tau(\hat{w}) := \left\{ j \in [d] : \hat{\Pi}_j \geq \tau \right\},$$

¹The probability simplex $\Delta_{|M^+|-1}$ consists of nonnegative weights w that sum to one: $\sum_{m \in M^+} w_m = 1$.

for some use-specified threshold τ . Similar to the standard argmax (without ties), $\text{ip}_\tau(\hat{w})$ only returns a collection of *variables*, which together constitute a single *model*. This selection procedure can be unstable if some marginal probabilities $\hat{\Pi}_j$ are near the threshold τ . It also may fail to adapt to relationships among variables (see Appendix A for an example).

2.3 Model selection stability

To assess the stability of \mathcal{M} , we measure how the output of \mathcal{M} changes with small perturbations to \mathcal{D} . We adapt the definition of stability in Soloff et al. (2024b) to the context of model selection.

Definition 2.1. A procedure \mathcal{M} has *model selection stability* $1 - \delta$ at sample size n if, for all datasets \mathcal{D} with n samples,

$$\frac{1}{n} \sum_{i=1}^n \mathbb{1}\{\hat{M} \cap \hat{M}^{\setminus i} = \emptyset\} \leq \delta, \quad (2)$$

where $\hat{M} = \mathcal{M}(\mathcal{D})$ and $\hat{M}^{\setminus i} = \mathcal{M}(\mathcal{D}^{\setminus i})$ for each $i \in [n]$.

In Definition 2.1, $\mathcal{D}^{\setminus i}$ refers to dataset \mathcal{D} with the i -th sample removed. In plain language, the inequality in (2) quantifies stability in terms of whether the sets of selected models overlap when we drop a single observation at random. Note that this notion of model selection stability holds for any “black box” model selection method of the form (1), in contrast to prior works that focus exclusively on variable selection (e.g., Meinshausen and Bühlmann (2010)).

3 Related work

Returning a model selection set. Returning a set of models to acknowledge inherent uncertainty in model selection is an old idea. Early literature on subset selection for linear regression (Spjøtvoll, 1972) focused on selecting the true model with high probability. More recent works extend the idea of a *model confidence set* to more general modeling settings (Hansen et al., 2011; Zhang et al., 2024). These works have a stochastic model for the data and construct a confidence set containing the best-fitting model with high probability. By contrast, our framework places no stochastic assumptions on the data, instead targeting a more modest goal of stability for the selected set.

Stability in variable selection. There is extensive literature on stability in variable selection; see, e.g., Khaire and Dhanalakshmi (2022) for a recent overview. Work in this area has overwhelmingly focused on “simple” procedures, returning a single subset of variables, and stability is measured by the degree of similarity of the selected subsets of variables. By contrast, Definition 2.1 is not satisfied by simple procedures unless they return the same model most of the time.

Bagging to improve stability. Bagging is an important tool for model selection and variable selection, and has been widely applied to stabilize model selection procedures (Breiman, 1996a;b). For example, *stability selection* thresholds the marginal bootstrap inclusion probabilities of each variable (Meinshausen and Bühlmann, 2010; Shah and Samworth, 2013). Additionally, *BayesBag* (Bühlmann, 2014) directly averages posterior distributions over different resamplings of the data. Huggins and Miller (2023) analyze the accuracy and stability properties of the BayesBag approach specifically for Bayesian model selection. Soloff et al. (2024a;c) shows that bagged weights are stable, meaning that dropping a single sample cannot change the bagged weights \hat{w} by much in the Euclidean norm. Bagging can thus express model uncertainty, but, as we show empirically in §5, selecting the most frequent model among multiple close contenders can still be quite unstable. In order to achieve any stability guarantees of the selected model(s), a new selection rule \mathcal{S} is needed, as discussed in §4.1.

Stabilizing classification. Our work builds on ideas from stable classification. Soloff et al. (2024b) introduces a framework for set-valued classification, combining the inflated argmax with bagging to guarantee stability for any base model selection method.

4 Our approach

We now provide a brief overview of our pipeline for stabilizing a model selection procedure $\mathcal{M} = \mathcal{S} \circ \mathcal{A}$.

1. First, we bag the weighting algorithm \mathcal{A} , i.e., average the weights fit on different random samples from \mathcal{D} . We fully define bagging in Algorithm 1.
2. Next, we pass the bagged weights \hat{w} through the *inflated argmax*, which selects a set of near-maximizers of \hat{w} that is robust to small perturbations of the weights. We define the inflated argmax for model selection in Definition 4.1.

In §4.2, we provide a stability guarantee for this pipeline that can be applied to any algorithm \mathcal{A} and any data set \mathcal{D} . We first discuss our pipeline in detail.

4.1 The inflated argmax for model selection

In this section, we propose an alternative selection procedure \mathcal{S} based on the inflated argmax. Soloff et al. (2024b) introduced the inflated argmax to guarantee stability in the context of multiclass classification. A key insight of this paper is that **if we formulate model selection as a multi-class classification problem, where each class corresponds to one of the candidate models, then we can directly use the inflated argmax and inherit its corresponding theoretical stability guarantees for model selection**. With this insight, the inflated argmax, an alternative model selection criteria \mathcal{S} that we denote by $\text{argmax}^\varepsilon$, will allow us to decide which subset \hat{M} of M^+ to return.

Definition 4.1 (Inflated argmax). For $m \in M^+$, let

$$R_m^\varepsilon = \left\{ w \in \Delta_{|M^+|-1} : w_m \geq \max_{m' \neq m} w_{m'} + \frac{\varepsilon}{\sqrt{2}} \right\}, \quad (3)$$

where $\Delta_{|M^+|-1}$ is a probability simplex. For any $w \in \Delta_{|M^+|-1}$ and $\varepsilon > 0$, the inflated argmax is defined as

$$\text{argmax}^\varepsilon(w) := \{m \in M^+ : \text{dist}(w, R_m^\varepsilon) < \varepsilon\}, \quad (4)$$

where $\text{dist}(w, R_m^\varepsilon) = \inf_{q \in R_m^\varepsilon} \|q - w\|$.

A visualization of a simple example of $\text{argmax}^\varepsilon$ where more than one model is returned is shown in Figure 1. An intuitive explanation of Definition 4.1 is that $m \in \text{argmax}^\varepsilon(w)$ indicates that m would have the largest weight in w by some margin if the weights w were slightly perturbed, where both the size of the margin and the weight perturbations scale with ε . This definition naturally allows for the number of returned models to adapt to the uncertainty in the model selection: for example, if the top two competing models are close in probability, then the inflated argmax will return both models for some choice of small ε . On the other hand, if the top two competing models have a large enough gap in their two weights, the inflated argmax will only return the top model for a choice of small ε .

The parameter ε is *not* something to be tuned. It is chosen to satisfy a user-specified stability tolerance; see §4.2.

4.2 Stability guarantee

In this section, we state a theorem guaranteeing the stability of our approach based on our definition of stability in Definition 2.1.

Theorem 4.2. (Adapted from Soloff et al. (2024b, Theorem 17).) For any model selection procedure $\mathcal{S} \circ \mathcal{A}$, our method $\text{argmax}^\varepsilon \circ \tilde{A}_{K,B}$ satisfies model selection stability at instability level

$$\delta = \frac{1}{\varepsilon^2} \left(1 - \frac{1}{|M^+|} \right) \left(\frac{1}{n-1} \frac{\rho}{1-\rho} + \frac{16e^2}{B} \right),$$

where $\rho = \frac{K}{n}$ for subbagging and $\rho = 1 - (1 - \frac{1}{n})^K$ for bagging.

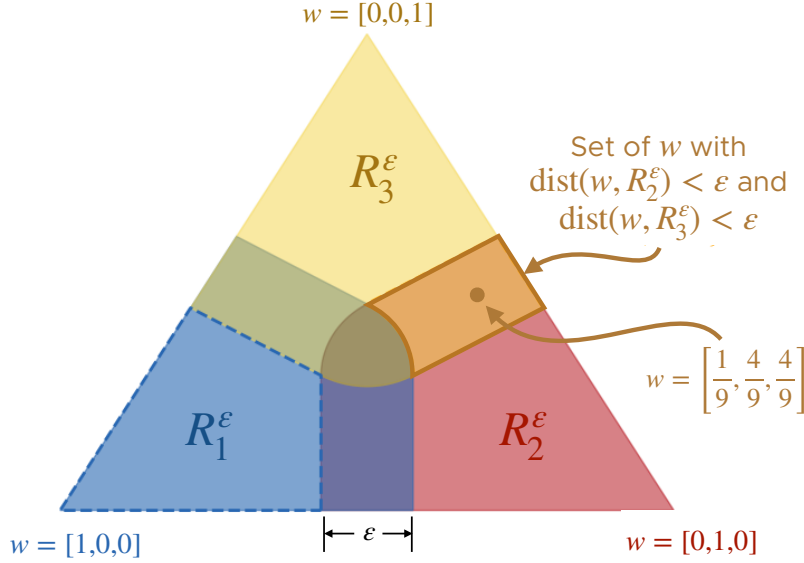


Figure 1: Visualization of argmax^ϵ when $|M^+| = 3$. The weights assigned to each model \mathcal{A} can be mapped onto a 3-dimensional probability simplex as shown. The example weight vector $w = [\frac{1}{9}, \frac{4}{9}, \frac{4}{9}]$ lands in an area that is within ϵ distance of regions R_2^ϵ and R_3^ϵ , which are the regions corresponding to returning models m_2 and m_3 , respectively. Because this weight vector is in an “uncertain” region based on ϵ for distinguishing whether model m_2 or m_3 provides a better fit to the data, argmax^ϵ will return both models: $\{m_2, m_3\}$. In contrast, weight vector $w = [\frac{1}{9}, \frac{1}{9}, \frac{7}{9}]$ would land in the area labeled R_3^ϵ , and argmax^ϵ will return m_3 only.

The main use for this theorem is that the user can choose a tolerable worst-case instability δ for their model selection, input the known parameters of the problem (i.e., $|M^+|$ candidate models, K samples per bag, n total samples, and B bags), and directly solve for the ϵ that should be used for argmax^ϵ .

Recall that ϵ determines how much we inflate the argmax, so when it’s smaller, the inflated argmax is closer to the standard argmax. Accordingly, when ϵ is smaller, Theorem 4.2 gives a larger δ , reflecting a weaker stability guarantee. Further, note that the instability level δ decreases (i.e., stability increases) by decreasing the bag size K and increasing the number B of bags. The size of our model class $|M^+|$ has only a small influence on the level of instability of our procedure. For example, when there are two models, $|M^+| = 2$, the factor $1 - \frac{1}{|M^+|} = \frac{1}{2}$, giving a constant-factor boost in stability over the case where M^+ is countably infinite, where $1 - \frac{1}{|M^+|}$ becomes 1.

This theoretical result is the first to provide theoretical guarantees for model selection stability that is agnostic to the underlying models, base algorithm, and data distribution.

5 Experiments

Our experiments assess and compare the stability of five different model selection approaches, described in Table 1.

We perform experiments in three settings: identifying important variables in a synthetic dataset that contains a small collection of highly correlated variables (see Appendix C), identifying the latent Lotka-Volterra governing differential equations from noisy trajectory data generated from these equations, and constructing a graph to represent cell-signaling pathways of 11 proteins. In the first two settings, we generate synthetic datasets for N trials, each contaminated with independent Gaussian noise, allowing us to examine the stability across a collection of datasets where we know the ground truth m^* .

NOTATION SELECTION CRITERION

$\text{argmax} \circ \mathcal{A}$	Model(s) with maximum weight assigned by \mathcal{A}
$\text{argmax} \circ \tilde{\mathcal{A}}_{K,B}$	Model(s) with maximum weight assigned by $\tilde{\mathcal{A}}_{K,B}$
$\text{top-}k \circ \tilde{\mathcal{A}}_{K,B}$	k models with k largest weights assigned by $\tilde{\mathcal{A}}_{K,B}$
$\text{ip}_\tau \circ \tilde{\mathcal{A}}_{K,B}$	Model with variables with inclusion probability $\geq \tau$ in $\tilde{\mathcal{A}}_{K,B}$
$\text{argmax}^\varepsilon \circ \tilde{\mathcal{A}}_{K,B}$	ε -inflated argmax of $\tilde{\mathcal{A}}_{K,B}$

Table 1: Table of notation for each model selection algorithm. \mathcal{A} refers to a base algorithm mapping a dataset \mathcal{D} to empirical predicted probabilities \hat{w} for each possible subset, and $\tilde{\mathcal{A}}_{K,B}$ is the subbagged version of \mathcal{A} for bags with K randomly selected (without replacement) samples.

In each experiment, we compute weights \hat{w} across the set candidate models M^+ using a base algorithm \mathcal{A} and a subbagged version of \mathcal{A} denoted $\tilde{\mathcal{A}}_{K,B}$. Based on (2), we compute the stability for trial $j \in [N]$ using

$$\delta_j = \frac{1}{n} \sum_{i=1}^n \mathbb{1}\{\hat{M}_j \cap \hat{M}_j^{\setminus i} = \emptyset\}, \quad (5)$$

This definition of stability measures, for trial j , the proportion of LOO selected models $\hat{M}_j^{\setminus i}$ for $i \in [n]$ that have no overlap with the set of selected models \hat{M}_j returned by training on the entire dataset. We also compute the empirical cumulative distribution function (CDF)

$$\frac{1}{N} \sum_{j=1}^N \mathbb{1}\{\delta_j \leq \delta\}, \quad (6)$$

as a function of $\delta \in [0, 1]$ to highlight variation across trials with different random seeds (shown in Figure 3 and Figure 7). Curves higher on the plot are better in the sense that the corresponding method achieves model selection stability δ (Definition 2.1) for a larger fraction of trials, and our primary interest is in small δ (i.e., high stability).

We additionally compute utility-weighted accuracy, inspired by Zaffalon et al. (2012), using

$$\frac{1}{N} \sum_{j=1}^N \frac{\mathbb{1}\{m^* \in \hat{M}_j\}}{|\hat{M}_j|}, \quad (7)$$

where m^* is the “true” data generating model in the synthetic experiments. This measure down-weights the accuracy by the number of models returned $|\hat{M}_j|$. This metric is used to compare methods in the center column of Figure 3.

5.1 Model discovery of Lotka-Volterra dynamics

This experiment focuses on discovering Lotka-Volterra dynamics from data using SINDy. The Lotka-Volterra equations were first derived to model chemical reactions in the seminal work (Lotka, 1910) and later studied in the now classic use case of predator-prey dynamics (Lotka, 1925). The Lotka-Volterra equations are

$$\dot{u}^{(1)}(t) = \alpha u^{(1)}(t) - \beta u^{(1)}(t)u^{(2)}(t), \quad (8a)$$

$$\dot{u}^{(2)}(t) = -\gamma u^{(2)}(t) + \zeta u^{(1)}(t)u^{(2)}(t), \quad (8b)$$

where $u^{(1)}$ is the population density of prey, $u^{(2)}$ is the population density of predators, $\dot{u}^{(1)}$ and $\dot{u}^{(2)}$ are the population growth rates, and t corresponds to time. The parameters $\alpha, \beta, \gamma, \zeta > 0$ respectively refer to the prey’s growth rate, the predator’s impact on the prey’s death rate, the predator’s death rate, and the prey’s impact on the predator’s growth rate (Lotka, 1925). We now imagine we do not know our system is governed by the Lotka-Volterra equations and wish to discover the governing model from data. Our concern is in recovering the correct terms rather than estimating the parameters.

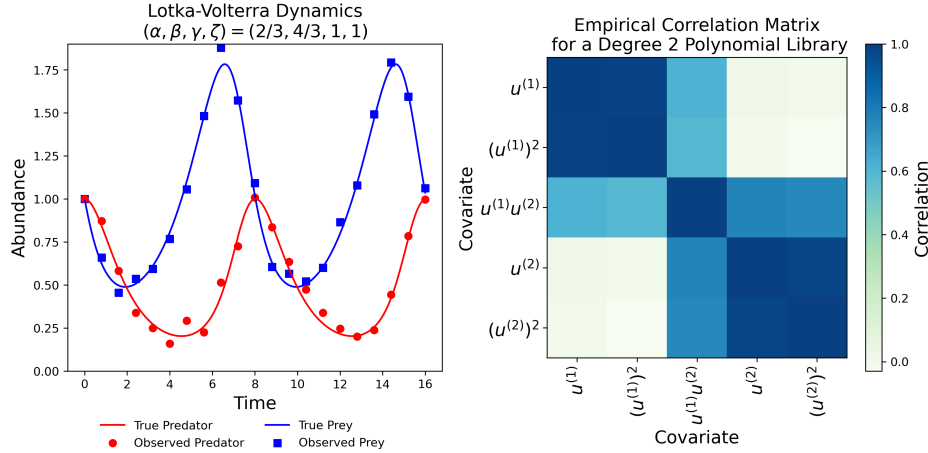


Figure 2: **(Left)** Lotka-Volterra trajectories for one simulated dataset. The time span ranges from 0 to 16, and there are 21 time points with predator-prey information contaminated with $\mathcal{N}(0, 0.05)$ distributed noise. **(Right)** Empirical correlation matrix for the variable library input into SINDy and E-SINDy. We use the library $(c, u^{(1)}, (u^{(2)})^2, u^{(1)}u^{(2)}, u^{(2)}, (u^{(2)})^2)$, where c is a constant.

5.1.1 Base algorithm \mathcal{A} : Sparse Identification of Nonlinear Dynamical Systems (SINDy)

One application of sparse regression is the discovery of governing equations of a system from observations. Specifically, we seek to learn the governing equations of a system of the form

$$\frac{d}{dt}u(t) = f(u(t)), \quad (9)$$

where $u(t) = [u^{(1)}(t), u^{(2)}(t), \dots, u^{(d)}(t)]^\top$ is a d -dimensional state vector containing quantities of interest at time t , and f is the function describing how the derivative of $u(t)$ evolves with time. The Sparse Identification of Nonlinear Dynamical Systems (SINDy, Brunton et al. (2016)) algorithm represents a differential equation of the form (9) as a weighted sum of terms in a library of functional forms,

$$\dot{u}(t) = \Theta(u)\Xi, \quad (10)$$

where $\Theta(u) \in \mathbb{R}^{n \times p}$ (n samples of p functionals) is the library of functionals of $u(t)$ (e.g., polynomial transformations), and $\Xi \in \mathbb{R}^{p \times d}$ are the fitted coefficients. Ξ is assumed to be sparse, so our goal is to find which elements of Ξ should be nonzero, which will immediately give the estimated structure of the governing equations. SINDy finds a sparse solution to Ξ by solving a sparse linear regression problem; see Appendix B for more details on sparse regression.

As a bagged extension of SINDy, Ensemble SINDy (E-SINDy, Fasel et al. (2022)) creates an ensemble of model fits, and with this ensemble, the final model is chosen via thresholding inclusion probabilities of each library term based on a tolerance τ . This approach corresponds to applying stability selection (Meinshausen and Bühlmann, 2010; Shah and Samworth, 2013) to SINDy, using sequentially thresholded ridge regression (STRidge, Rudy et al. (2017)) instead of the LASSO for \mathcal{A} . E-SINDy aggregates the coefficients by selecting covariates whose inclusion probability is greater than some prespecified value $\tau \in (0, 1)$. Of the variables with an inclusion probability greater than τ , the corresponding coefficients are set to the average fitted values across bags. The collection of variables with a nonzero coefficient correspond to the selected model. In our experiments, we refer to this ensemble approach as $\text{ip}_\tau \circ \tilde{\mathcal{A}}_{K,B}$, where the base algorithm \mathcal{A} is SINDy.

5.1.2 Data generation

We generate synthetic datasets containing $n = 21$ time points of abundance data for predator and prey populations, solve from the Lotka-Volterra equations and contaminate with Gaussian noise. This data is

generated to match key characteristics of a real world predator-prey dataset from the Hudson Bay Company (Hewitt, 1921) in terms of the periodicity of observations in relation to the dynamics. $N = 100$ trials (i.e., independent datasets) are independently generated according to the same data generation process. We provide further details of this data generation process in Appendix D.1. We visualize one set of trajectories in Figure 2.

To construct our library of functions, we selected degree-two polynomials as our covariates, and for one dataset, we visualize the corresponding covariate correlations in Figure 2. As seen in the correlation matrix, the covariate structure contains highly correlated variables (e.g., $u^{(1)}$ and $(u^{(1)})^2$), which impacts the model selection stability of SINDy.

In our experiments, we solve the linear regression problem with the STRidge penalization (Rudy et al., 2017) as our base algorithm \mathcal{A} , as in Fasel et al. (2022).

5.1.3 Results

We see that across various choices of ε , the inflated argmax provides enhanced stability while at the same time yielding small and accurate sets of selected model(s). This boost in utility-weighted accuracy is due to the adaptivity of the inflated argmax: this method will output a single model as often as possible, whereas for example, top- k will always output k model selections, leading to a comparatively lower utility in many cases. This point is further confirmed in the plot of the median number of models returned vs. worst-case instability in Figure 3.

For a fixed level of worst-case instability empirically seen, we can visualize the empirical CDF to assess the distribution of instability values δ_j across trials $j \in [N]$. We see in Figure 3 that the inflated argmax provides a distribution of instability values much closer to 0 (i.e., higher stability) compared to all other conventional approaches investigated.

In summary, Figure 3 shows that (a) selection methods that return a single model (argmax and ip_τ , even with subagging the base algorithm) are less stable than methods that return one or more selected models (i.e., the inflated argmax and top- k), (b) the inflated argmax provides higher utility-weighted accuracy scores for similar worst-case stability levels as top- k , meaning that the inflated argmax is returning smaller sets containing the correct model more often and (c) the inflated argmax provides smaller sets of returned models compared to top- k for a wide range of worst-case stability values.

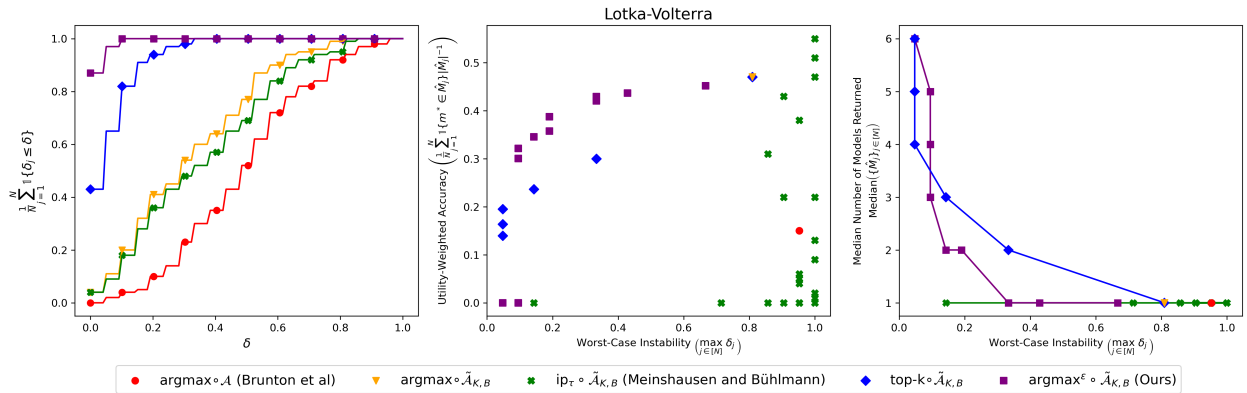


Figure 3: Lotka-Volterra results. **(Left column)** Empirical CDF for the stability measures δ_j , computed in (5), across $j \in [N]$ for each \mathcal{S} . We chose the parameters $\tau = 0.63$, $k = 2$, and $\varepsilon = 0.09$ since these values yield a utility-weighted accuracy of approximately 0.3 for each \mathcal{S} . **(Center column)** Utility-weighted accuracy, computed in (7), versus the worst-case instability across δ_j . **(Right column)** Median number of models returned across j versus the maximum δ_j across $j \in [N]$ for each \mathcal{S} . **(Center and right columns)** We plot the range of values $k \in [1, \dots, 6]$, and $\varepsilon \in (0, 1)$ and $\tau \in (0, 1)$ with approximately evenly spread values across their supports.

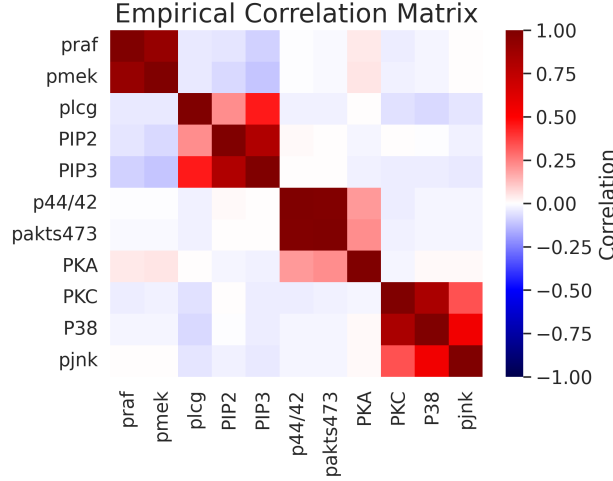


Figure 4: Empirical correlation matrix of the 11 proteins. Data from Sachs et al. (2005).

5.2 Graph selection on flow cytometry data

We consider a model selection problem where the model to select is the sparse connection structure within a graph. The base algorithm \mathcal{A} we consider for this problem is the Graphical LASSO (gLASSO), which is developed in Friedman et al. (2008). The gLASSO estimates the structure of a graph by performing a maximum likelihood estimation of the precision matrix Θ subject to an l_1 penalty of the estimated precision matrix. More precisely, the gLASSO assumes the data $x_i \sim \mathcal{N}(0, \Theta^{-1})$, where $x_i \in \mathbb{R}^d$ across samples $i \in [n]$, and finds an estimate $\hat{\Theta}$ such that

$$\hat{\Theta} = \underset{\Theta}{\operatorname{argmax}} \log \det \Theta - \operatorname{tr}(\tilde{\Sigma}\Theta) - \lambda \|\Theta\|_1, \quad (11)$$

where $\|\cdot\|_1$ is the entry-wise l_1 norm, $\operatorname{tr}(\cdot)$ is the trace, $\tilde{\Sigma}$ is the sample covariance matrix, and λ is the penalization hyperparameter. In our experiments, we select λ via cross-validation, as described in §D.2.1, and hold this quantity fixed across our experiments.

We compute LOO stability results from a flow cytometry dataset in Sachs et al. (2005) (labeled “cd3cd28icam2+u0126”), containing $d = 11$ proteins (nodes) and $n = 759$ cells (samples). Figure 4 shows the empirical correlation structure of these 11 proteins in this dataset, which clearly shows grouped relationships among proteins.

SELECTION METHOD	LOO INSTABILITY	AVG. LOO SET SIZE
$\operatorname{argmax} \circ \mathcal{A}$	0.453	1.00
$\operatorname{ip}_{0.5} \circ \tilde{\mathcal{A}}_{K,B}$	0.013	1.00
$\operatorname{argmax} \circ \tilde{\mathcal{A}}_{K,B}$	0.112	1.00
$\operatorname{top-2} \circ \tilde{\mathcal{A}}_{K,B}$	0.008	2.00
$\operatorname{argmax}^{0.02} \circ \tilde{\mathcal{A}}_{K,B}$ (Ours)	0.008	1.58

Table 2: Table of stability and the average number of model structures returned across LOO trials for selecting the structure of the inverse precision matrix for a flow cytometry dataset taken from Sachs et al. (2005). In this experiment, \mathcal{A} is the graphical LASSO (Friedman et al., 2008), $\tilde{\mathcal{A}}_{K,B}$ is the bootstrapped graphical LASSO with $B = 10,000$ and $K = 700$.

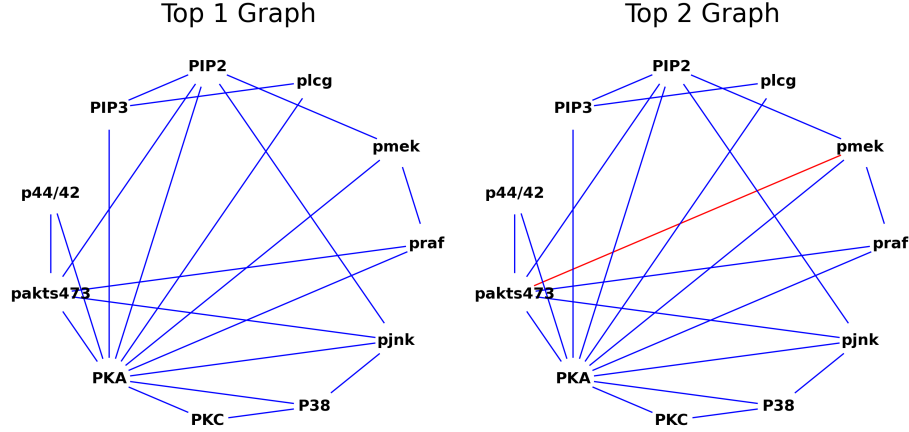


Figure 5: Visualization of the top two graph structures selected via subbagged gLASSO with 10,000 bags. The red connection shown in the right graph highlights that this connection is the only difference between the top 1 and top 2 selected graph structures. The top 1 graph was selected for 9.31% of bags, and the top 2 graph was selected for 8.54% of bags.

5.2.1 Results

Since we have one dataset to compute the LOO stability, $N = 1$. We compute stability results for the algorithms gLASSO (\mathcal{A}) and subbagged gLASSO ($\tilde{\mathcal{A}}_{K,B}$), where $K = 700$ and $B = 10,000$, for the selection methods argmax , $\text{ip}_{0.5}$, top-2, and $\text{argmax}^{0.02}$. The value for ε for the inflated argmax was chosen so that the LOO instability closely matched the LOO instability of top-2, and τ in ip_τ was chosen so that the number of selected connections was approximately the same as the number of connections given by the top selected subbagged graph. These results are shown in Table 2.

As seen in Table 2, our method, $\text{argmax}^{0.02}$, provides the lowest LOO instability while minimizing the average number of graphs selected across the 759 LOO model fits. We also note that the percentage of model fits on bags that resulted in the top 2 models shown in 5 are relatively close: 9.31% for the top graph structure versus 8.54% for the second most selected graph structure, which suggests a reasonable degree of uncertainty in the “best” model. Due to this uncertainty in the selected model, selection methods that return only one model (i.e., argmax and ip_τ) cannot sufficiently account for this uncertainty in the top model. Since the top two graph structures differ by one connection, this kind of result can provide evidence for follow up experiments, for example, to elucidate the relationship between the pakts473 and pmek proteins.

6 Discussion

The combination of bagging and the inflated argmax described in this paper can be applied to any black-box model selection procedure and offer stability guarantees described in Theorem 4.2. We define a notion of stability that is distinct from other works, one that computes the proportion of LOO selected models that are disjoint from the selection made by training on the full data. This is in contrast to, for example, *covariate-level* stability in linear models.

Our experiments illustrate that, in addition to providing theoretical stability guarantees, our method outperforms *ad hoc* procedures. Specifically, choosing the most frequently selected model across bags (i.e., $\text{argmax} \circ \tilde{\mathcal{A}}_{K,B}$) provides limited stability gains relative to an unstable base algorithm. Selecting the top- k models across bags enhances stability but is not adaptive to the underlying empirical uncertainty of the model selection process; k models will always be returned to the user. Choosing the returned model based on marginal inclusion probabilities (ip_τ) of individual covariates is limited to covariate stability tasks and presents hyperparameter selection challenges (i.e., how to select τ). In contrast, the inflated argmax *adapts*

to the number of models returned based on the underlying uncertainty, provides an approach for empirically protecting against a worst-case instability, and provides competitive utility-weighted accuracies (i.e., returns the correct model in the smallest possible \hat{M}). Our framework provides multiple opportunities for further investigation, including exploring the interplay of stable model selection and identifiability, as well as stabilizing model selection without bagging, therefore reducing computation.

References

- Breiman, L. (1996a). Bagging predictors. *Machine Learning*, 24:123–140.
- Breiman, L. (1996b). Heuristics of instability and stabilization in model selection. *The Annals of Statistics*, 24(6):2350 – 2383.
- Breiman, L., Friedman, J., Olshen, R. A., and Stone, C. J. (1984). *Classification and Regression Trees*. Chapman and Hall/CRC, 1 edition.
- Brunton, S. L., Proctor, J. L., and Kutz, J. N. (2016). Discovering governing equations from data by sparse identification of nonlinear dynamical systems. *Proceedings of the National Academy of Sciences of the United States of America*, 113(15):3932–3937.
- Bühlmann, P. (2014). Discussion of big Bayes stories and BayesBag. *Statistical science*, 29(1):91–94.
- de Silva, B., Champion, K., Quade, M., Loiseau, J.-C., Kutz, J., and Brunton, S. (2020). Pysindy: A python package for the sparse identification of nonlinear dynamical systems from data. *Journal of Open Source Software*, 5(49):2104.
- Drton, M. and Perlman, M. D. (2004). Model selection for Gaussian concentration graphs. *Biometrika*, 91(3):591–602.
- Effrosynidis, D. and Arampatzis, A. (2021). An evaluation of feature selection methods for environmental data. *Ecological Informatics*, 61:101224.
- Fasel, U., Kutz, J. N., Brunton, B. W., and Brunton, S. L. (2022). Ensemble-sindy: Robust sparse model discovery in the low-data, high-noise limit, with active learning and control. *Proceedings of the Royal Society A: Mathematical, Physical and Engineering Sciences*, 478(2260):20210904.
- Friedman, J., Hastie, T., and Tibshirani, R. (2008). Sparse inverse covariance estimation with the graphical lasso. *Biostatistics*, 9(3):432–441.
- Hansen, P. R., Lunde, A., and Nason, J. M. (2011). The model confidence set. *Econometrica*, 79(2):453–497.
- Hewitt, C. G. (1921). *The conservation of the wild life of Canada*. C. Scribner’s Sons, New York.
- Hoerl, A. E. and Kennard, R. W. (1970). Ridge regression: Biased estimation for nonorthogonal problems. *Technometrics*, 12(1):55–67.
- Huggins, J. H. and Miller, J. W. (2023). Reproducible Model Selection Using Bagged Posteriors. *Bayesian Analysis*, 18(1):79–104.
- Kaptanoglu, A. A., de Silva, B. M., Fasel, U., Kaheman, K., Goldschmidt, A. J., Callahan, J., Delahunt, C. B., Nicolaou, Z. G., Champion, K., Loiseau, J.-C., Kutz, J. N., and Brunton, S. L. (2022). Pysindy: A comprehensive python package for robust sparse system identification. *Journal of Open Source Software*, 7(69):3994.
- Khaire, U. M. and Dhanalakshmi, R. (2022). Stability of feature selection algorithm: A review. *Journal of King Saud University - Computer and Information Sciences*, 34(4):1060–1073.
- Lotka, A. J. (1910). Contribution to the theory of periodic reactions. *The Journal of Physical Chemistry*, 14(3):271–274.

- Lotka, A. J. (1925). *Elements of Physical Biology*. Williams and Wilkins Company, Baltimore, Maryland.
- Masini, R. P., Medeiros, M. C., and Mendes, E. F. (2023). Machine learning advances for time series forecasting. *Journal of economic surveys*, 37(1):76–111.
- Meinshausen, N. and Bühlmann, P. (2010). Stability selection. *Journal of the Royal Statistical Society Series B: Statistical Methodology*, 72(4):417–473.
- Petzold, L. (1983). Automatic selection of methods for solving stiff and nonstiff systems of ordinary differential equations. *SIAM Journal on Scientific and Statistical Computing*, 4(1):136–148.
- Rudy, S. H., Brunton, S. L., Proctor, J. L., and Kutz, J. N. (2017). Data-driven discovery of partial differential equations. *Science Advances*, 3(4):1–6.
- Sachs, K., Perez, O., Pe’er, D., Lauffenburger, D. A., and Nolan, G. P. (2005). Causal protein-signaling networks derived from multiparameter single-cell data. *Science*, 308(5721):523–529.
- Saeys, Y., Inza, I., and Larrañaga, P. (2007). A review of feature selection techniques in bioinformatics. *Bioinformatics*, 23(19):2507–2517.
- Shah, R. D. and Samworth, R. J. (2013). Variable selection with error control: another look at stability selection. *Journal of the Royal Statistical Society: Series B (Statistical Methodology)*, 75(1):55–80.
- Soloff, J. A., Barber, R. F., and Willett, R. (2024a). Bagging provides assumption-free stability. *Journal of Machine Learning Research*, 25(131):1–35.
- Soloff, J. A., Barber, R. F., and Willett, R. (2024b). Building a stable classifier with the inflated argmax. In *The Thirty-eighth Annual Conference on Neural Information Processing Systems*.
- Soloff, J. A., Barber, R. F., and Willett, R. (2024c). Stability via resampling: statistical problems beyond the real line. *arXiv preprint arXiv:2405.09511*.
- Spjøtvoll, E. (1972). Multiple comparison of regression functions. *The Annals of Mathematical Statistics*, 43(4):1076–1088.
- Tibshirani, R. (1996). Regression shrinkage and selection via the lasso. *Journal of the Royal Statistical Society. Series B (Methodological)*, 58(1):267–288.
- Veslavov, I. C. and Stumpf, M. P. (2020). Decision tree models and cell fate choice. *bioRxiv*.
- Vrieze, S. I. (2012). Model selection and psychological theory: a discussion of the differences between the Akaike information criterion (AIC) and the Bayesian information criterion (BIC). *Psychological methods*, 17(2):228–243.
- Yu, B. (2013). Stability. *Bernoulli*, 19(4):1484–1500.
- Zaffalon, M., Corani, G., and Mauá, D. (2012). Evaluating credal classifiers by utility-discounted predictive accuracy. *International Journal of Approximate Reasoning*, 53(8):1282–1301.
- Zhang, T., Lee, H., and Lei, J. (2024). Winners with confidence: Discrete argmin inference with an application to model selection. *arXiv preprint arXiv:2408.02060*.

A Example: Linear regression with correlated covariates

Consider the setting in which we have a set of covariates $x = [x^{(1)}, x^{(2)}, \dots, x^{(d)}]^\top$ where

$$\mathbb{E}[Y|X = x] = x^{(1)} + x^{(3)}, \quad (12)$$

and we seek to learn this relationship using sparse variable selection. If $x^{(1)}$ is highly correlated with $x^{(2)}$, and $x^{(3)}$ is highly correlated with $x^{(4)}$ and $x^{(5)}$ (see covariance matrix in Figure 6), then subtle changes in the dataset could result in selecting any of the following models $m_k(\mathbf{x})$:

$$\begin{aligned} m_1(\mathbf{x}) &= \{x^{(1)}, x^{(3)}\}, & m_2(\mathbf{x}) &= \{x^{(1)}, x^{(4)}\}, \\ m_3(\mathbf{x}) &= \{x^{(1)}, x^{(5)}\}, & m_4(\mathbf{x}) &= \{x^{(2)}, x^{(3)}\}, \\ m_5(\mathbf{x}) &= \{x^{(2)}, x^{(4)}\}, & m_6(\mathbf{x}) &= \{x^{(2)}, x^{(5)}\}. \end{aligned} \quad (13)$$

If each of the six models above were selected with approximately equal frequency across bags, the output of Algorithm 1, would be approximately

$$\hat{w} \approx (1/6) [1, 1, 1, 1, 1, 0, 0, \dots]. \quad (14)$$

A selection method that finds the argmax of \hat{w} would be unstable despite the stability of \hat{w} derived from bagging. We seek a method that outputs models corresponding to selected variable sets

$$\left\{ \{x^{(1)}, x^{(2)}\} \times \{x^{(3)}, x^{(4)}, x^{(5)}\} \right\}, \quad (15)$$

accurately indicating that our method suggests either x_1 or x_2 should be included in the selected model, but not necessarily both. In other words, this output reflects the fact that our model selection method cannot reliably distinguish among the six models in (13).

Limitations of the argmax. The argmax applied to \hat{w} in (14) will be highly sensitive to small perturbations in \hat{w} . Furthermore, the single best model does not reflect the inherent uncertainty in the model selection and that several models are almost equally likely.

Limitations of top- k . If the user chooses $k = 2$, only 2 models will be returned to the user, which does not reflect that any of the 6 models are approximately equally likely. This failure to adapt to uncertainty also applies to the other direction: if the user chooses $k > 6$, top- k will still give back k models, despite the fact that only 6 are highly likely.

Limitations of stability selection The stability selection method (Meinshausen and Bühlmann, 2010) will select the model corresponding to selected variables $\{x^{(1)}, x^{(2)}, x^{(3)}, x^{(4)}, x^{(5)}\}$ if τ is sufficiently small. This result can be misleading, in that it ultimately selects a model with five selected covariates as opposed to indicating that we lack certainty about which of multiple two-covariate models is correct.

Benefits of the inflated argmax. For a large enough choice of ε , the $\text{argmax}^\varepsilon$ would return all 6 models in (13). This output can be reported as a Boolean expression as in (15), which accurately reflects the uncertainty in the model selection.

B Variable selection in linear models with LASSO

In the linear case, the data is modeled as the form

$$y_i = \langle x_i, \beta \rangle + \eta_i, \quad \eta_i \sim N(0, \sigma^2), \quad (16)$$

where $\sigma^2 \in \mathbb{R}$ is a vector containing the response error variance, and $\beta \in \mathbb{R}^d$ is the vector of regression coefficients. In many practical settings, the true population β is hypothesized to be sparse, and the goal is to accurately estimate which elements of β are nonzero.

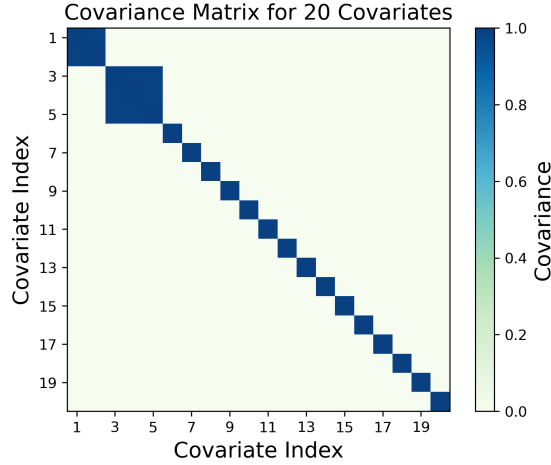


Figure 6: Covariance matrix for each simulated dataset. Covariate indices 1 and 3 were used to construct the response y .

Consider the following common model selection approach: first solve the *least absolute shrinkage and selection operator* (LASSO, Tibshirani (1996)) problem

$$\hat{\beta} = \operatorname{argmin}_{\beta} \left\{ \frac{1}{n} \sum_{i=1}^n (y_i - \langle x_i, \beta \rangle)^2 + \lambda R(\beta) \right\}, \quad (17)$$

where λ is a hyperparameter controlling the sparsity of β , and the regularization term $R(\beta) = \|\beta\|_1$. Then select variables via

$$\hat{m}(\mathcal{D}) = \mathbb{1}\{|\hat{\beta}| > 0\} \quad (18)$$

where $\hat{\beta}$ implicitly depends on the dataset \mathcal{D} . In this context, the LASSO provides unstable model selections, particularly in settings with nontrivial correlations among covariates (Meinshausen and Bühlmann, 2010). Moreover, since many variable selection algorithms, including the LASSO, only return a single set of selected covariates, these methods do not directly provide an approach for assessing uncertainty in the selected model.

C Experiment: Penalized linear regression experiment with highly correlated covariates

This experiment is based on the motivating example in (12), where we have two important covariates and a small collection of highly correlated covariates.

C.1 Data generation

In our standard regression example, we simulate datasets for $j \in [N]$ trials, where $N = 200$, according to the following process:

$$x_i \sim \mathcal{N}(0, C), \quad (19)$$

where $x_i \in \mathbb{R}^d$, \mathcal{N} denotes a Normal distribution, and $C \in \mathbb{R}^{d \times d}$ is visualized in Figure 6. Figure 6 visualizes the covariance structure of the 20 covariates in the design matrix X , where the nonzero covariance between distinct covariates is 0.99, corresponding to extremely correlated covariates. For a single trial j , we simulate a dataset with $d = 20$ covariates and $i \in [n]$ samples. We take the first and third columns as the covariates used to create the response y ,

$$y_i = x_i^{(1)} + x_i^{(3)} + v_i, \quad v_i \sim \mathcal{N}(0, 0.3^2), \quad (20)$$

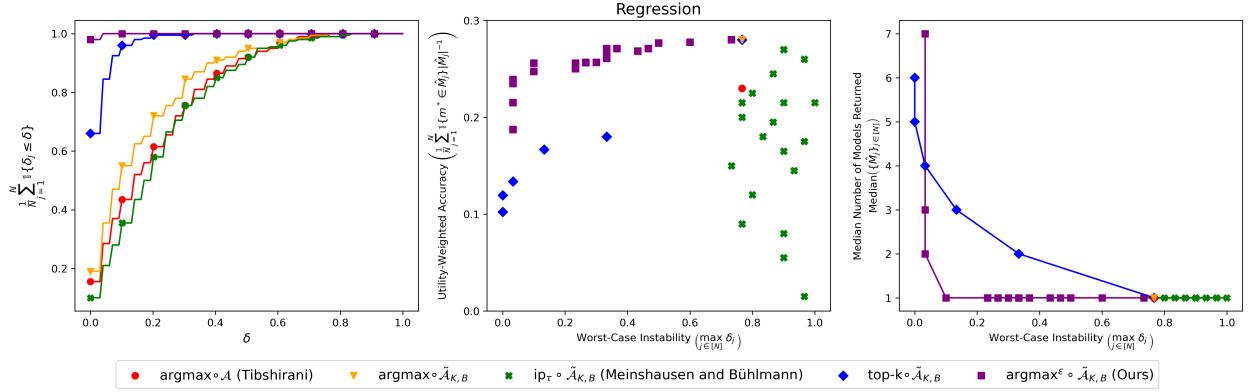


Figure 7: Regression results. In the left plot, we plot the stability curves for the parameters $\tau = 0.3$, $k = 2$, and $\varepsilon = 0.8$ since these values yield a utility-weighted accuracy of approximately 0.18 for each \mathcal{S} . **(Left column)** Empirical CDF for the stability measures δ_j , computed in (5), across $j \in [N]$ for each \mathcal{S} . **(Center column)** Utility-weighted accuracy, computed in (7), versus the worst-case instability across δ_j . **(Right column)** Median number of models returned across j versus the maximum δ_j across $j \in [N]$ for each \mathcal{S} . **(Center and right columns)** We plot the values $k \in [1, \dots, 6]$, and $\epsilon \in (0, 1)$ and $\tau \in (0, 1)$ with approximately evenly spread values across their supports.

where $\beta = [1, 1]^\top$, $x_i^{(1)}$ and $x_i^{(3)}$ are respectively the first and third covariates for sample i , and v_i represents independent Gaussian distributed observation noise with mean 0 and standard deviation 0.3 for sample i .

We solve each optimization problem (i.e., fits on the full datasets \mathcal{D} , LOO datasets $\mathcal{D}^{\setminus i}$ for $i \in [n]$, and bags \mathcal{D}^b for $b \in [B]$ across trials $j \in [N]$) for $\hat{\beta}$ using the optimization function in (17) for $R(\beta) = \|\beta\|_1$, which is equivalent to the LASSO.

C.1.1 Optimization hyperparameter

Selecting λ via cross-validation leads to much denser models than the ground truth model, so we increase λ to a level that induced more sparsity. This approach implicitly assumes we have prior knowledge of approximately how many coefficients are important in the regression task, but not necessarily which are important. We select $\lambda = 0.5$ since this penalization level led to highly sparse variable selections. We note, however, that the theory behind the inflated argmax is *model agnostic*, meaning that stability guarantees apply for any choice of λ .

C.2 Small sample size ($n = 30$)

We generate independent datasets (i.e., trials) for a small sample size, $n = 30$. For each of the $N = 200$ trials, we generate a dataset with $d = 20$ covariates and $n = 30$ training samples.

C.2.1 Base algorithm \mathcal{A} : LASSO

Our learning algorithm \mathcal{A} is the LASSO, which corresponds to solving (17) with $R(\beta) = \|\beta\|_1$, and $\tilde{\mathcal{A}}_{K,B}$ corresponds to a subbagged LASSO with $B = 10,000$ bags and $K = 25$ training samples per bag.

C.2.2 Results

Figure 7 provides an empirical CDF of δ (6), the utility-weighted accuracy (7) versus the empirical worst-case instability, and the median number of sets returned across N trials versus the worse-case instability. The empirical CDF across our chosen selection methods \mathcal{S} show that the selection methods that return a single model, the argmax and ip_τ , are the least stable. Subbagging, which helps in stabilizing the estimated weights \hat{w} assigned to each model m , yields marginal gains in stability when using the argmax. Top- k and

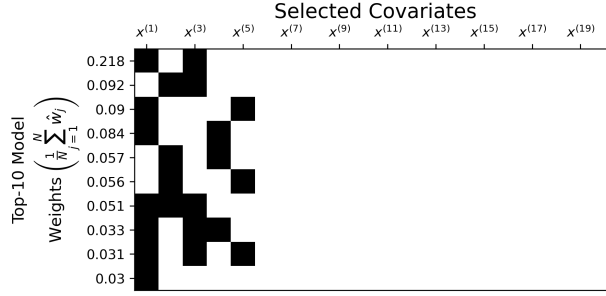


Figure 8: Top-10 selected models with their corresponding weights $\frac{1}{N} \sum_{j=1}^N \hat{w}_m^{(j)}$, which averages the weights across trials. Selected covariates for each model are shown with a black square.

the inflated argmax, on the other hand, provide enhanced stability due to the fact that these methods are able to return more than one model. The ip_τ selection method fails to control the worst-case instability across a variety values of τ , but is able to achieve good utility-weighted accuracy. Top- k is able to achieve good utility-weighted accuracy with stable estimates. However, the inflated argmax is able to attain similar stability as top- k , while achieving a higher utility-weighted accuracy across a range of stability levels.

We confirm that the inflated argmax frequently outputs a single model by plotting the median number of models returned compared to the worst-case instability across various choices of ε compared to various choices of k .

To illustrate that returning multiple models, when necessary, can be represented compactly, we borrow notation from logic to express an example of 6 models, reported in Figure 8. Figure 8 shows that the model weights averaged across trials $\left(\frac{1}{N} \sum_{j=1}^N \hat{w}^{(j)}\right)$. The top 6 models can be reported as

$$\left\{ \{x^{(1)}, x^{(2)}\} \times \{x^{(3)}, x^{(4)}, x^{(5)}\} \right\}$$

which succinctly describes the model options.

C.3 Larger sample size ($n = 300$)

To illustrate the utility of the inflated argmax in a setting where this method is particularly useful, we construct an example where the model weights \hat{w} estimated via bootstrapping suggest a high level of uncertainty in the model selection. We focus on one trial, so $N = 1$. In constructing this example, we follow a similar procedure as described in (19) and (20). We set $d = 200$, $n = 300$, $B = 10,000$, $K = 25$, $\lambda = 0.5$, and $v_i \sim N(0, 0.5^2)$, where 0.5 is the response error standard deviation for each sample i . The correlation structure of covariates is extended to 200 covariates, where similarly the first 5 covariates are highly correlated with a correlation of 0.99 as in Figure 6, and $x^{(1)}$ and $x^{(3)}$ are used to construct y with $\beta = [1, 1]^\top$.

Figure 9 shows the selections of among the first 5 covariates out of the 200 total for the top-10 models (covariates 6 through 200 are not selected in any of the top-10 models) using the full dataset versus a LOO dataset. As an illustrative example, we choose a LOO dataset that yielded a different top model compared to the top model using the full dataset.

The model weights clearly show uncertainty in the selection since the weights estimated for each of the top-10 models are very close together, suggesting that small perturbations of the dataset could impact the top model selected. The empirical stability for $\text{argmax}_0 \hat{\mathcal{A}}_{K,B}$ using (5) yields $\delta_j = 0.14$ for this one trial j . This result means that 14% of the time in our 300 LOO trials, when a single sample was removed from the full dataset, a model other than $\{x^{(2)}, x^{(3)}\}$ (the model selected using all 300 samples) was selected.

The inflated argmax, on the other hand, will select more than one model in this instance for relatively small ε due to the large uncertainty in the model weights. To concretely show this result, we compute the inflated argmax’s model selection(s) and choose ε using the result in Theorem 4.2. Setting δ to a fixed value, we can

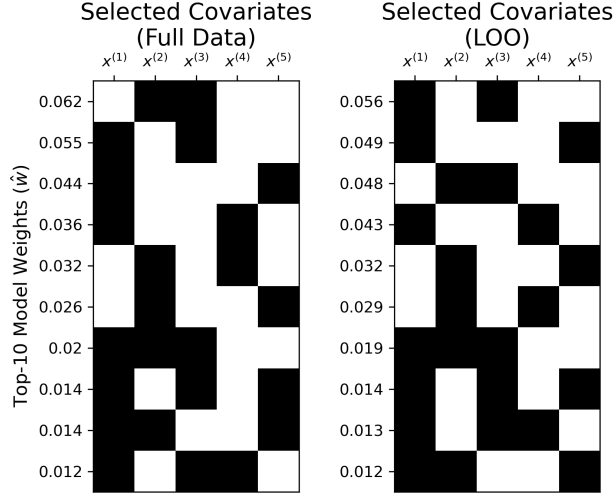


Figure 9: Models with the top 10 largest weights assigned via subbagging with $B = 10,000$ bags for one trial. The y-axis labels correspond to the model weights estimated with 10,000 bags. Covariates within each model (row) that were selected to have a nonzero estimated coefficient by LASSO are shown in black, and covariates that were not selected are shown in white. Only the first 5 covariates are shown since the top 10 models did not select covariates any of the covariates $x^{(6)}, x^{(7)}, \dots, x^{(200)}$. **(Left)** Top-10 models using the full dataset where $n = 300$. **(Right)** Top-10 models using a LOO dataset where $n - 1 = 299$.

compute ε via the following expression for subbagging

$$\varepsilon = \sqrt{\frac{1}{\delta} \left(\frac{1}{n-1} \frac{K/n}{1-K/n} \right)}. \quad (21)$$

Since $|M^+| = 2^{200}$, we set $\frac{1}{|M^+|}$ to 0. Additionally, since the Monte-Carlo error term $\frac{16e^2}{B}$ is known to be overly conservative, and since we use a large number of bags B in this experiment, we set this term equal to 0 as well. With $n = 300$, $K = 25$, and $\delta = 0.05$, we compute that $\varepsilon = 0.078$.

The instability of $\arg\max^{0.078} \circ \tilde{\mathcal{A}}_{K,B}$ is 0, meaning that for 0% of the 300 leave-one-out datasets, the inflated $\arg\max$ returned a completely disjoint model selection. Additionally, the inflated $\arg\max$ returned 6 models, which correspond to

$$\left\{ \{x^{(1)}, x^{(2)}\} \times \{x^{(3)}, x^{(4)}, x^{(5)}\} \right\}.$$

This set of returned models is very reasonable given the underlying correlation structure among the covariates.

Moreover, the type of stability in this work only measures changes the stability due to LOO changes to the dataset, which is a relatively small perturbation to the data. In reality, a method would ideally provide robustness to more substantial changes in the dataset (e.g., providing the same, or approximately the same, model selection(s) with a different dataset drawn from the same underlying distribution). The inflated $\arg\max$ is better equipped than the $\arg\max$ in this scenario by returning six models, reflecting the large uncertainty in selecting a model.

D Main experimental details

In our experiments, we utilize a cluster computing system to distribute parallel jobs across CPU nodes.

D.1 Lotka-Volterra simulations

This section provides further details of the experiment in §5.1. We utilize the `pysindy` Python package (Kaptanoglu et al., 2022; de Silva et al., 2020) for their implementations of these methods to perform out Lotka-Volterra experiments with SINDy.

D.1.1 Data generation

We generate data from the Lotka-Volterra differential equations described in (8) for $(\alpha, \beta, \gamma, \zeta) = (2/3, 4/3, 1, 1)$ for 21 evenly spread time points t in the range $t \in [0, 16]$ and initial condition $[1, 1]^\top$. Solutions of this ordinary differential equation were obtained with the LSODA (Petzold, 1983) solver. For each $t \in (0, 16]$, non-inclusive of the initial condition, we contaminate each $u^{(1)}(t)$ and $u^{(2)}(t)$ with $\mathcal{N}(0, 0.05^2)$ Gaussian noise, where 0.05 is the standard deviation of the measurement noise level.

To obtain sparse solutions of the regression problem and therefore estimate the governing equations, we solve the optimization problem with STRidge (Rudy et al., 2017), which iteratively (a) solves the equation in (17) with $R(\beta) = \|\beta\|^2$, corresponding to solving Ridge regression (Hoerl and Kennard, 1970), and (b) thresholds $\hat{\beta}$ based on ω , where ω is the minimum magnitude needed for a coefficient in the weight vector. Any coefficient with an estimated magnitude below ω is set to 0. This process is repeated until a convergence criterion is met.

D.1.2 Cross-validating optimization hyperparameters

We perform a grid search across two parameters to find a combination that leads to a low validation MSE. The 5-fold validation MSE is measured as

$$\text{val-MSE}(\lambda, \omega; 5) = \frac{1}{5|\mathcal{V}(v)|} \sum_{v=1}^5 \sum_{t \in \mathcal{V}(v)} \|\hat{u}(t; \lambda, \omega) - u(t)\|^2, \quad (22)$$

where $\mathcal{V}(v)$ is the collection of time points included in the validation evaluation for fold $v \in 1, 2, \dots, 5$; $\hat{u}(t; \lambda, \omega)$ is a vector of solutions, containing $\hat{u}^{(1)}(t; \lambda, \omega)$ and $\hat{u}^{(2)}(t; \lambda, \omega)$, to the model selected by SINDy using optimization parameters λ and ω at time t ; $u(t)$ is a vector of the observed values for $u^{(1)}(t)$ and $u^{(2)}(t)$ at time t . The trajectories were temporally split into 5 disjoint sets, where each set contains temporally adjacent time points.

	ω					
λ	0.16	0.17	0.18	0.19	0.20	0.25
0.0075	0.0538	0.0538	0.0539	0.0982	0.0963	0.1156
0.01	0.0538	0.0538	0.0538	0.0981	0.0963	0.1942
0.02	0.1285	0.1285	0.1287	0.1275	0.1256	0.4403
0.03	0.1285	0.1285	0.3160	0.3166	0.3202	0.3451
0.15	0.0788	-	-	-	-	-
1	-	-	-	10.65	-	14.94

Table 3: Table of hyperparameter combinations and corresponding validation MSEs for choosing the STRidge λ and ω hyperparameters. Any combination of hyperparameter values that led to a null model (selecting none of the covariates to include in the model) for any of the validation folds is reported as “-”. We choose the hyperparameter combination that should give sparser models (larger λ and larger ω) in the case of tied validation MSE, which leads us to choose $\lambda = 0.01$ and $\omega = 0.18$ (bolded and highlighted).

We provide a table of validation MSEs averaged across the 5 folds in Table 3. Given our discretization of λ and ω values, we choose $\omega = 0.18$ and $\lambda = 0.01$ and keep these values fixed in our experiments presented in Appendix C. Figure 10 visualizes the corresponding model selected by 5-fold cross validation. The best

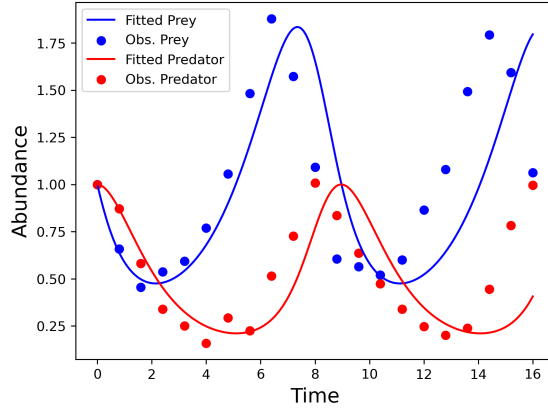


Figure 10: Lotka-Volterra solutions (solid lines) for the equations selected using SINDy with hyperparameters $\lambda = 0.01$ and $\omega = 0.18$ using one observational dataset (points).

estimated model is

$$\dot{u}^{(1)} = 0.636u^{(1)} + -1.255u^{(1)}u^{(2)}, \quad (23)$$

$$\dot{u}^{(2)} = -0.839u^{(2)} + 0.833u^{(1)}u^{(2)}, \quad (24)$$

which selects the correct terms in each differential equation with low error on the fitted $\hat{\beta}$ coefficients.

D.2 Graph subset selection

D.2.1 Cross-validation to select λ

We select the penalization hyperparameter λ in (11) via 5-fold cross-validation. The validation log-likelihood averaged across the 5 folds is computed as

$$\text{val-log-likelihood}(\lambda; 5) = \frac{1}{5} \sum_{v=1}^5 \left(\log \det \hat{\Theta}_v - \text{tr}(\tilde{\Sigma}_v \hat{\Theta}_v) - \lambda \|\hat{\Theta}_v\|_1 \right), \quad (25)$$

where $\hat{\Theta}_v$ is computed by solving (11) using the *training* data in fold index v , and $\tilde{\Sigma}_v$ is the sample covariance matrix computed from the *validation* data in fold index v . Computing (25) on the flow cytometry data across various choices of $\lambda \in [1, \dots, 500]$ yields the curve shown in Figure 11. Based on this figure, the best choice of λ is $\lambda = 77$, which we keep constant throughout our experiments in §5.2.1.

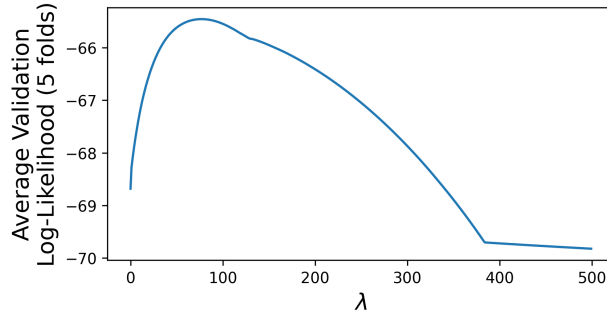


Figure 11: Average 5-fold validation log-likelihood across different choices of λ . The λ that maximizes the log-likelihood averaged over 5 held-out validation folds is $\lambda = 77$.

E Stability with varying numbers of bags

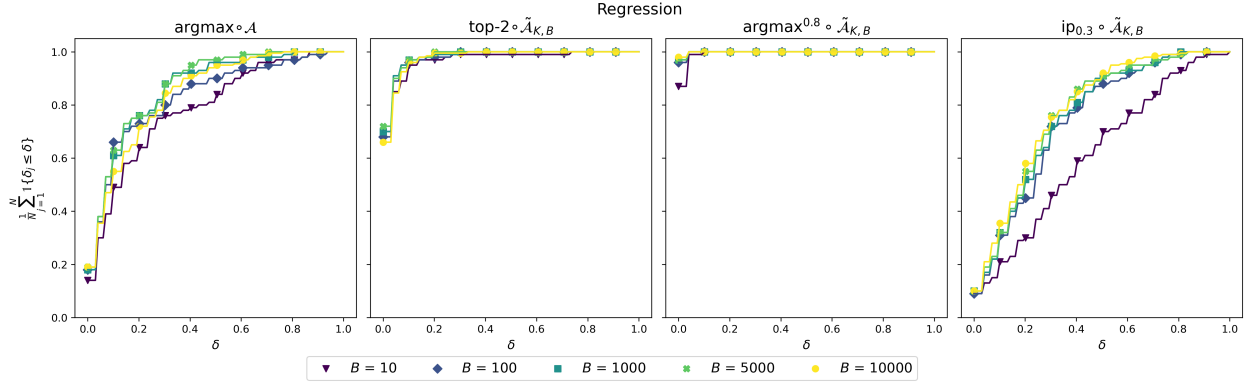


Figure 12: Empirical CDF of instability measures δ_j across trials $j \in [N]$ in the regression experiment for varying number of bags B across four different selection methods: the argmax, top-2, $\text{argmax}^{0.8}$, $\text{ip}_{0.3}$. The values of k , ε , and τ were chosen to be consistent with the CDF plot in Figure 7.

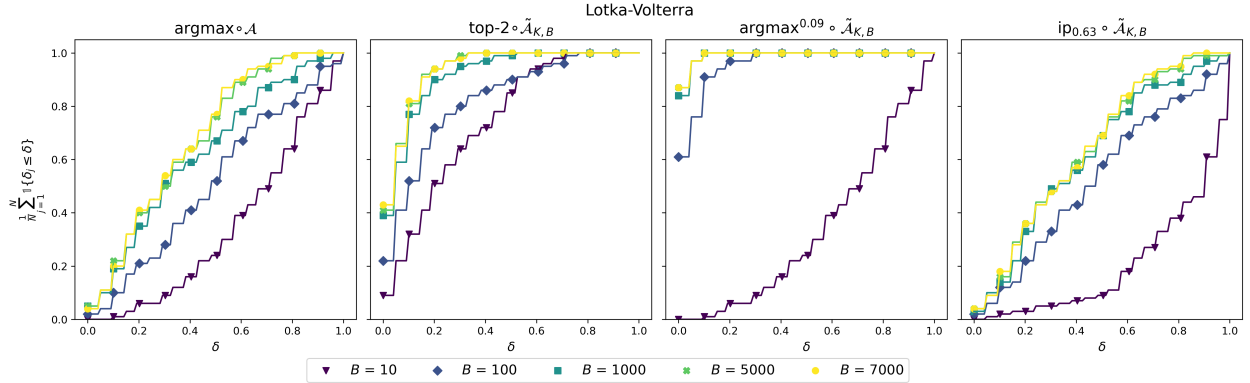


Figure 13: Empirical CDF of instability measures δ_j across trials $j \in [N]$ in the Lotka-Volterra experiment for varying number of bags B across four different selection methods: the argmax, top-2, $\text{argmax}^{0.09}$, $\text{ip}_{0.63}$. The values of k , ε , and τ were chosen to be consistent with the CDF plot in Figure 3.

The computational complexity of estimating the weights associated with each possible model $m \in M^+$ is not determined by the cardinality of the set M^+ , but rather the number of bags B used to estimate the weights associated with each model. Intuitively, we can generally expect that a larger number of bags (i.e., larger B) will correspond to a better estimate of the weights \hat{w} for each model m across selection methods. Figures 12 and 13 visualize the empirical CDF of instabilities δ_j across trials $j \in [N]$, where $N = 200$ in the regression experiments and $N = 100$ in the Lotka-Volterra experiment. A separate line is plotted for each choice of B .

In both plots, we see that $B = 10$ provides the least stability, evidenced by the larger proportion of δ_j s near $\delta = 1$. The regression example provides evidence that generally, increasing the number of bags improves stability. However, this plot does not appear to clearly evidence this hypothesis as well as the Lotka-Volterra experiment. We hypothesize that since the covariates are highly correlated in the regression example with many reasonable models able to accurately predict the response, this setting may yield more variable stability results across the number of bags compared to the Lotka-Volterra example, which has a clear, unique model.

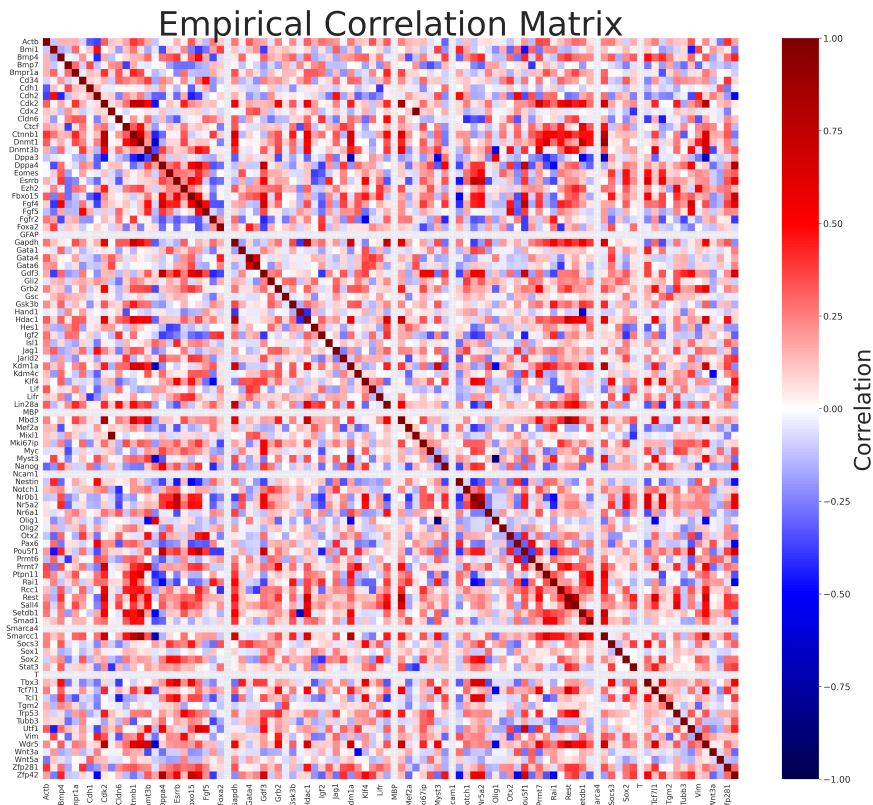


Figure 14: Empirical correlation matrix of gene expression across 50 cells from data in Veleslavov and Stumpf (2020). Rows and columns that show a null value correspond to genes that showed no variability in expression across the 50 cells.

F Decision tree classification on single cell transcriptomics data

We investigate a model selection problem involving deciding the structure of a decision tree for multiclass classification. In this setting, we only measure two decision trees as distinct from each other if the trees split on the same features for a given split. Therefore, we do not consider the exact split value for continuous features in deciding whether two selected models are the same.

We explore the decision tree stability with data from single cell transcriptomics to classify stem cell fate based on gene expression. Mouse embryonic stem cells were sequenced for their gene expression and subsequently labeled as three different cell types: embryonic stem cells (ESC), epiblast-like intermediate cells (EPI), and neural progenitor cells (NPC) (Veleslavov and Stumpf, 2020). The cell fate label is noted to be assigned by clustering, so there is uncertainty in the true cell type label.

The dataset contains 547 cells and 96 gene expression values per cell. To explore stability in a setting where the sample size is much lower than the feature dimensionality, which is a common problem in genetics, we randomly subsample the number of cells to 50 and compute decision tree stabilities. As shown in Figure 14, gene expression is high correlation among genes, which may lead to instabilities in the fitted decision tree for small perturbations in the training data.

The base algorithm \mathcal{A} corresponds to a multiclass classification tree. Broadly, decision trees create a sequence of splits on features that sort the training data samples into nodes, where a particular split is chosen to minimize the impurity of the samples in the two split nodes. Greedy algorithms are typically implemented to sequentially choose the locally best split at each node. More information on decision trees can be found in Breiman et al. (1984).

For this classification problem, we choose to measure dissimilarities among samples in a node via Gini impurity, which can be written as

$$\sum_{d=1}^D p_{ld}(1 - p_{ld}) \quad (26)$$

for $d \in [D]$ classes at node l , where the proportion of class d in node l is

$$p_{ld} = \frac{1}{n_l} \sum_{y \in Q_l} \mathbb{I}\{y = d\}, \quad (27)$$

and Q_l denotes the split of node l based on feature index f and split value t_l :

$$Q_l^{\text{left}} = \{(x, y) \mid x_f \leq t_l\}, \quad (28)$$

$$Q_l^{\text{right}} = Q_l \setminus Q_l^{\text{left}}. \quad (29)$$

Our experiments use the default hyper-parameters in the `sklearn.tree.DecisionTreeClassifier` function.

F.1 Results

Since we have one dataset of gene expression across cells, $N = 1$ in this example. Table 4 shows the stability results and average number of models returned across LOO trials. Notably, ip_τ is absent from this table because this selection method is specific to variable selection, which is a special class of model selection.

Based on Table 4, significant instabilities are seen for both the $\text{argmax} \circ \mathcal{A}$ and $\text{argmax} \circ \tilde{\mathcal{A}}_{K,B}$ model selection methods, while $\text{top-2} \circ \tilde{\mathcal{A}}_{K,B}$ provides enhanced stability. For the inflated argmax , we chose $\varepsilon = 0.03$ so that the stability matched that of the stability of top-2 in order for us to directly compare the number of returned models. For a fixed level of instability $\delta = 0.12$, the inflated argmax returns a smaller number of models on average across LOO trials, showing that our method adaptively returns the smallest set of models based on the underlying uncertainty in the selection.

For $\varepsilon = 0.04$, we obtain 0.04 instability, corresponding to a high degree of stability with a LOO average of 2.88 returned models. We visualize the top 3 selected models across bootstrap samples in Figure 15. From these trees, we can see that the first and second most common selected trees across bootstrap samples are completely disjoint, potentially indicating strong correlations among the features for both trees. However, the third most commonly selected tree differs from the top tree by only one split, suggesting there may be a high correlation between the gene expressions of *Lin28a* and *Nanog*. Future investigations can focus on disentangling the associations among the genes selected in the top tree versus the second most selected tree to elucidate their associations with the cell fates.

SELECTION METHOD	LOO INSTABILITY	AVG. LOO SET SIZE
$\text{argmax} \circ \mathcal{A}$	0.40	1.00
$\text{argmax} \circ \tilde{\mathcal{A}}_{K,B}$	0.24	1.00
$\text{top-2} \circ \tilde{\mathcal{A}}_{K,B}$	0.12	2.02
(Ours) $\text{argmax}^{0.03} \circ \tilde{\mathcal{A}}_{K,B}$	0.12	1.74

Table 4: Table of stability and the average number of models returned across LOO trials for selecting the structure of the multi-class decision tree for a gene expression dataset from Veleslavov and Stumpf (2020). In this experiment, \mathcal{A} is a classification decision tree, and $\tilde{\mathcal{A}}_{K,B}$ is a bootstrapped classification decision tree with $B = 10,000$ and $K = 45$. In computing the returned models, if there is an exact tie in the top models, all ties are returned, which explains why top-2 returns slightly more than 2 models on average across the LOO fits.

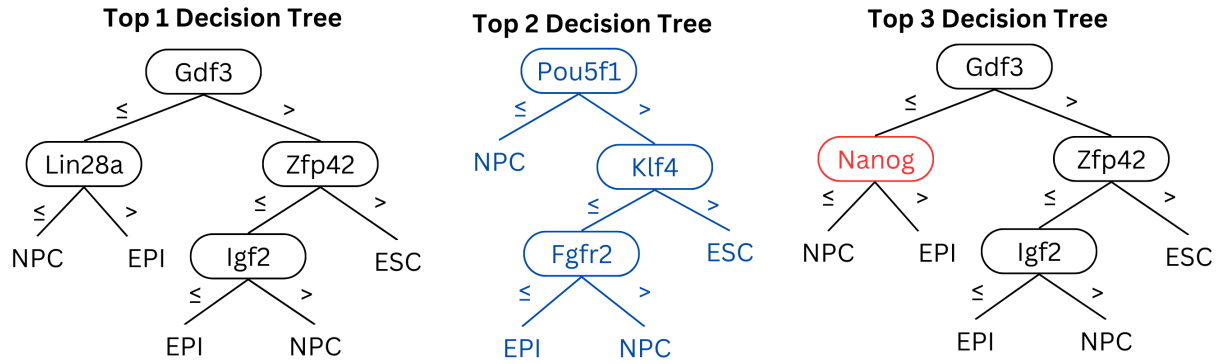


Figure 15: Visualization of the decision tree structures for the top 2 trees chosen by bootstrap sampling the data for $K = 45$ samples per bag across $B = 10,000$ bags. Differences between the top and second tree are indicated in blue in the second tree, and the differences between the first and third trees are indicated in red. The names of the genes that determine the split at each node are shown in ovals, and the class labels NPC, ESC, and EPI are listed for each leaf. The top 1 decision tree was selected by 4.74% of bags, the top 2 decision tree was selected by 2.80% of bags, and the third decision tree was selected by 2.24% of bags. The exact values used for the splits at each node were not considered in our stability results.